Energy 55 (2013) 226–235

Contents lists available at SciVerse ScienceDirect

Energy

journal homepage: www.elsevier.com/locate/energy

# Performance evaluation and experiment system for waste heat recovery of diesel engine

Gao Wenzhi*, Zhai Junmeng, Li Guanghua, Bian Qiang, Feng Liming

*State Key Laboratory of Engines, Tianjin University, Tianjin 300072, China*

ARTICLE INFO

*Article history:*
Received 18 July 2012
Received in revised form
5 March 2013
Accepted 24 March 2013
Available online 11 May 2013

*Keywords:*
Diesel engine
Waste heat recovery
Reciprocating piston expander

ABSTRACT

In this paper, a waste heat recovery system is proposed where a high speed turbocharged diesel engine acts as the topper of a combined cycle with exhaust gases used for a bottoming Rankine cycle. The paper describes a mathematical model to evaluate the performance of Rankine cycle system with a reciprocating piston expander. The paper focuses on the performance evaluation and parameter selection of the heat exchanger and reciprocating piston expander that are suitable to waste heat recovery of ICE (internal combustion engine). The paper also describes the experimental setup and the preliminary results. The simulation results show that a proper intake pressure should be 4–5 MPa at its given mass flow rate of 0.015–0.021 kg/s depending on the waste heat recovery of a turbocharged diesel engine (80 kW/2590 rpm). The net power and net power rise rate at various ICE rotation speeds are calculated. The result shows that introducing heat recovery system can increase the engine power output by 12%, when diesel engine operates at 80 kW/2590 rpm. The preliminary experimental results indirectly prove the simulation model by two negative work loops in the *P*–*V* curve, under a low intake pressure and steam flow rate condition.



## 1. Introduction

The world population and industrial activity increased considerably during the 20th century, and consequently, energy consumption during this period had risen almost exponentially. This increased energy consumption, largely fulfilled by fossil fuels, has resulted in significant environmental problems. The latest reports on the environmental contamination and the exhaustion of the resources showed that the pollution levels went up due to the intensive use of the internal combustion engines, and for this reason human beings are looking for more efficient and clean sources to produce motive and electric power [1,2]. For an internal combustion engine, significant amount of heat is released to the environment in forms of exhaust and cooling water. The high quality of the energy in the engine exhaust gases suggests that it is possible to further considerably increase ICE efficiency by converting exhaust heat to mechanical energy. Further improvements in fuel conversion efficiency require a recovery cycle system to recover various losses encountered in the ICE [3,4].

In 1970s, the idea of heat recovery with Rankine cycle in the automotive internal combustion engines was first conceived [5], but it was overlooked due to complication and the loss in power to weight ratios that would be inevitably resulted. Recent technical progress has made the idea realizable. Using a Rankine bottoming cycle, operating on the exhaust waste heat, is becoming an effective and practical method for improving the global efficiency of internal combustion engines. Lacopo Vaja and Agostino Gambarotta [6] described a specific thermodynamic analysis in order to efficiently match a vapor cycle to that of a stationary internal combustion engine. In the paper the best fluid and cycle configuration was to be employed, the main parameters of the thermodynamic cycles and the overall efficiency of the combined power system were determined. The analysis demonstrated that a 12% increase in the overall efficiency can be achieved with respect to the engine with no bottoming. Rody Ei Chammas et al. [7] proposed a system to recover the exhaust heat based on Rankine cycle using turbine expander. They analyzed and compared the advantages offered by a Rankine system designed for hybrid vehicles when water, R-245ca, isopentane is employed as working fluid. The authors believed ORCs (organic Rankine cycle) provide an attractive combination of efficiency and affordability for engine exhaust WHR. Ho Teng et al. [8] discussed the possibility of using supercritical dry-type organic Rankine cycle for waste heat recovery in heavy duty diesel engines.

* Corresponding author. Tel.: +86 022 27407623 8024; fax: +86 022 27404244.
*E-mail address:* gaowenzhi@tju.edu.cn (G. Wenzhi).

0360-5442/$ – see front matter 
http://dx.doi.org/10.1016/j.energy.2013.03.073

In the paper, the quantity and quality of exhaust energy were evaluated in first law and second law of thermodynamics. The heat gains by the working fluid in the Charge air cooler (CAC), LT-EGR cooler, exhaust cooler, and HT-EGR cooler, and potential mechanical work output by employing the supercritical ORC-WHR system were calculated. The study demonstrated that 20% of the shaft power was obtained from a properly designed WHR system. Arias et al. [9] presented a theoretical study of different strategies of waste heat recovery in an internal combustion engine, operating in a hybrid vehicle (spark ignition engine and electric motor). The constant load conditions for the SI-engine in the hybrid vehicle were administrated a potential advantage for the implementation of a heat recovery system. Srinivasan et al. [10] studied the exhaust waste heat recovery from a dual fuel low temperature combustion engine using an Organic Rankine Cycle. Potential improvements in fuel conversion efficiency (FCE) and specific emissions ($NO_x$ and $CO_2$) with hot exhaust gas recirculation (EGR) and ORC turbo-compounding were quantified over a range of injection timings and engine loads. With hot EGR and ORC turbo-compounding, FCE was improved by an average of 7 percentage points for all injection timings and loads while $NO_x$ and $CO_2$ emissions were recorded with an 18 percent (average) decrease. Wang et al. [11] designed a dual loop ORC system which combined a high-temperature (HT) loop and a low temperature (LT) loop to simultaneously recover the waste heat from the exhaust and the coolant of a gasoline engine. They mainly describe the issue on the working fluids selection. Maogang He et al. [12] proposed a combined thermodynamic cycle for waste heat recovery of ICE, the cycle consisted of the organic Rankine cycle (ORC) for recovering the waste heat of lubricant and high-temperature exhaust gas.

The expander is commonly known as one of the key parts in recovery system of Rankine cycle, performance of the Rankine cycle system strongly depends on expanders. The choice of the expander strongly depends on the operating conditions and the size of the system. Two main types of machines can be distinguished: the turbo and positive displacement types. The literature mentioned above mostly use turbo-expander. But for a waste heat recovery of a medium internal combustion engine, the displacement type machines are more appropriate due to the small-scale Rankine cycle units. This expander is characterized by lower flow rates, higher-pressure ratios and much lower rotational speeds than turbo-machines [13]. Available options of volumetric expanders include reciprocating and rotary expanders, but rotary expanders, which are often based on the Wankel concept [13,14], show implementation difficulties, while reciprocating piston expanders result in an easier design and construction [15]. The steam flow rate come from ICE waste heat recovery is small, therefore the reciprocating piston expander is chosen as the expander of the Rankine cycle system.

The objective of this study is to investigate, through simulations and experiments, the combined effects of heat exchangers and reciprocating expander on the performance of Rankine cycle system. The paper describes the implementation approaches of Rankine cycle system that should fulfill a good performance and be most suitable for waste heat recovery of ICE.

## 2. Rankine cycle system for waste heat recovery

Heat recovery from the exhausts of an internal combustion engine, on the purpose of producing additional mechanical or electrical energy, can be accomplished by means of a suitably designed Rankine cycle. This section describes the Rankine cycle system that can be used to recover exhaust heat from ICE. Fig. 1 shows the Rankine cycle system. As shown in this figure, the working fluid passing through high pressure feed pump is sent into preheater and is preheated firstly, then it is carried through a number of parallel small-diameter tubes and is heated by the hot gas, when the ICE exhaust gas enters in the shell surrounding the tubes. The preheated working fluid is vaporized and superheated in evaporator/superheater, and the produced high pressure steam is sent to a single-stage reciprocating piston expander which is connected to an asynchronous electrical generator to convert mechanical to electrical power. The exhaust steam flowing out of the expander is condensed and water is pumped back into the heat exchanger by the feed water pump.

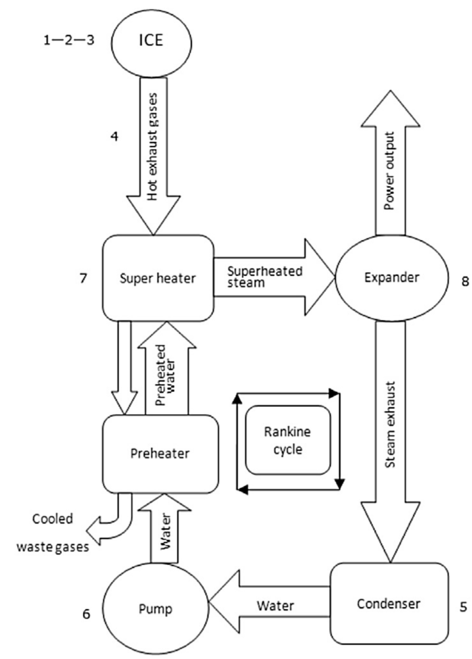


**Fig. 1.** Rankine cycle system.

In the combined cycle, Rankine cycle system is actually used to recover exhaust heat from ICE, which implies that the Rankine bottoming cycle is added to enhance the performances of a diesel engine. The graph plotted in Fig. 2 shows the thermodynamic cycle on the $T$–$S$ diagram for the combined cycle. Cycle I (1–2–3–4–1) refers to a diesel cycle and cycle II (5–6–7–8–5) refers to a Rankine cycle. The heat comes from ICE exhaust gases is used to heat the working fluid in the Rankine cycle, and the working fluid is heated and then becomes a superheated steam in the process 7–8. It is evident that the temperature at 8 is lower than the temperature at 4, which means the initial temperature of overheated steam is limited by the exhaust temperature.

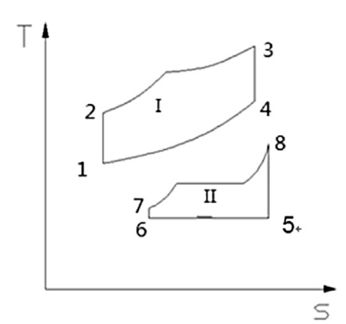


**Fig. 2.** $T$–$S$ diagram of combined cycle.

**Table 1**
Initial input parameters.

| Fluid | Tube side (water/steam) | Shell side (exhaust gases) |
|---|---|---|
| Entrance temperature (°C) | 95 | 533 |
| Outlet temperature (°C) | 300 (steam) | 200 |
| Operating pressure (MPa) | 5 | 0.1 |
| Flow rate (kg/s) | 0.022 | 0.177 |

## 3. Heat exchanger parameters

Heat exchanger performance depends on several parameters such as the heat exchanger structure, transfer area and temperature difference between hot gas and working fluid. In this paper, shell and tube heat exchangers are chosen as the preheater and evaporator. The shell contains the tube bundle, the exhaust gases flow over the tubes in multiple passes while the higher-pressure fluid is circulated in the tubes. In order to estimate the economic effect of the thermodynamic cycle optimization, the parameters of the heat exchangers, have to be determined. In the heat exchanger design process, a mean temperature difference method is used. The design steps are as follows:

1) Calculate the heat loads of the preheating, evaporation and superheating sections and the mass flow rate of working fluid on either side of exchanger according to the design requirements.
2) Ascertain the characteristic temperatures and physical parameters.
3) Calculate the mean temperature difference of each section.
4) Preliminarily design the heat transfer coefficient of each section, and calculate the initial area of heat transfer $F$.
5) Design the exchanger structure with the initial heat transfer area.
6) Calculate the heat transfer coefficient and the area of heat transfer $F'$, if $F'$ is close to $F$, then go on next step, if not, back to step 4) and recalculate them.
7) Calculate the tube-side and shell-side flow resistances.

The initial conditions of heat exchanger design are shown in Table 1. And heat transfer and fluid's temperature at each node are showed in Table 2.

With the information in Tables 1 and 2, the final heat exchanger parameters are determined using the method mentioned above and shown in Table 3.

## 4. Reciprocating piston expander

Performance of the Rankine cycle system strongly correlates with those of the expander. The choice of the machine strongly depends on the operating conditions and size of the system. Two main types of machines can be distinguished: the turbo and positive displacement types. The displacement type machines are more appropriate to the small-scale Rankine cycle units, because they are characterized by lower flow rates, higher-pressure ratios and much lower rotational speeds than turbo-machines. Since steam flow rate depending on ICE waste heat recovery is very small, so the reciprocating steam engine is chosen as the expander of the Rankine cycle system.

**Table 2**
Start-stop parameters each heat transfer section.

| Working fluid | | | Water/steam | Exhaust gas |
|---|---|---|---|---|
| Section | Heat transfer (kW) | Position node | Temperature (°C) | Temperature (°C) |
| Preheating | 7.86 | Inlet | 95 | 244 |
| | | Outlet | 170 | 200 |
| Evaporation | 49.96 | Inlet | 170 | 518 |
| | | Outlet | 170 | 244 |
| Superheating | 2.85 | Inlet | 170 | 533 |
| | | Outlet | 300 | 518 |

**Table 3**
Obtained heater parameters.

| | |
|---|---|
| Heat transfer area ($m^2$) | 18 |
| Pressure drop in the shell side (Pa) | 5451 |
| Tube inner diameter (mm) | 8 |
| Tube outer diameter (mm) | 10 |
| Tube number | 200 |
| Shell diameter (mm) | 165 |

### 4.1. Thermodynamic model of a reciprocating steam engine

A mathematical model of reciprocating steam engine is developed to research the performance of the steam engine. The model is based on the following equations.

Energy conservation equation:

$$\frac{dU}{dt} = \frac{dQ}{dt} - \frac{dW}{dt} + \sum \frac{dH}{dt} \tag{1}$$

where $U$ is the internal energy of the steam in the expander, $Q$ is the heat transferred to the steam in the expander, $W$ is the work done by the steam expansion, and $H$ is the stagnation enthalpy of steam flowing into and out of expander. Using $U = mu$ and $H = mh$, Eq. (1) may be written as

$$m\frac{du}{dt} + u\frac{dm}{dt} = \sum \frac{dQ_j}{dt} - p\frac{dV}{dt} + h_{in}\frac{dm_{in}}{dt} - h_{out}\frac{dm_{out}}{dt} \tag{2}$$

where $u$ is the specific internal energy of the steam in the expander, $Q_j$ is the heat losses from the steam to the expander walls or to expander head, $p$ and $V$ are the pressure and volume of the steam in the cylinder, respectively, $h_{in}$ and $h_{out}$ are respectively the specific enthalpy entering and leaving the cylinder, $m_{in}$ and $m_{out}$ are the mass entering and leaving the cylinder, respectively, and $m$ is the steam mass in the cylinder.

For the compression and expansion process, Eq. (2) is expressed as:

$$\frac{du}{dt} = \left(\sum \frac{dQ_j}{dt} - p\frac{dV}{dt} - u\frac{dm}{dt}\right) \Big/ m \tag{3}$$

Mass conservation equation:

$$\frac{dm}{dt} = \frac{dm_{in}}{dt} - \frac{dm_{out}}{dt} \tag{4}$$

Gas state equation:

The steam state is considered as real gas. Since the steam in cylinder is in saturated or superheated state, there is a functional

**Table 4**
Main parameters of the steam engine.

| | |
|---|---|
| Cylinder number | 1 |
| Total displacement (L) | 0.418 |
| Intake pressure (MPa) | 2 |
| Intake temperature (°C) | 300 |
| Outlet pressure (MPa) | 0.1 |
| Compression ratio | 19 |
| Crankshaft angle in admission | −10 to 50 TDC |
| Crankshaft angle in exhaust | −30 to 160 BDC |

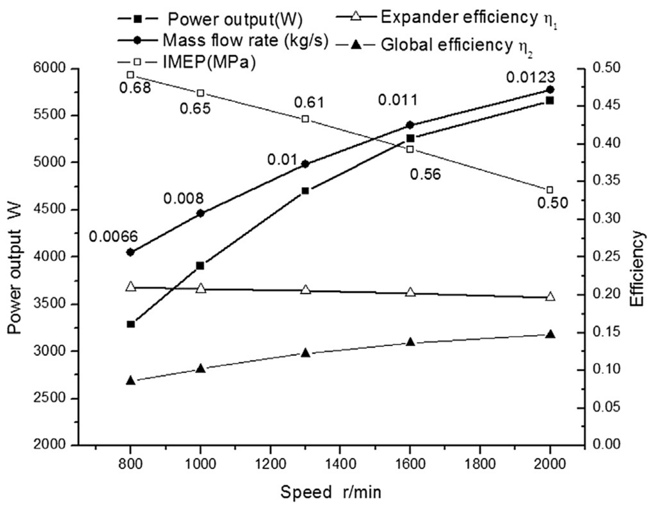


**Fig. 3.** Power output, expander efficiency, global efficiency and mass flow rate, IMEP vs. expander speed.

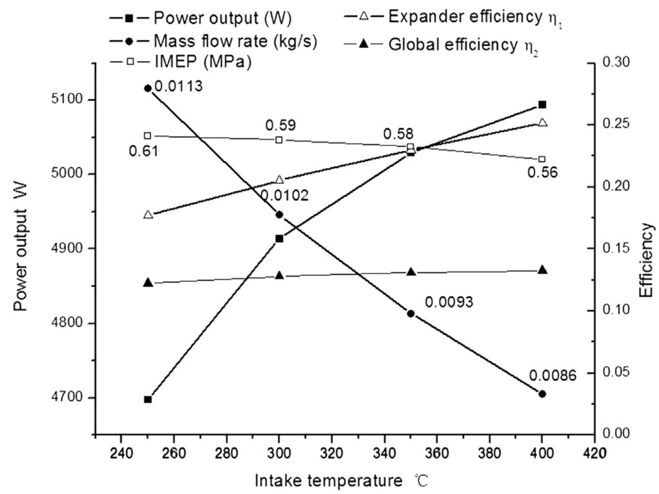


**Fig. 5.** Power output, expander efficiency, global efficiency and mass flow rate, IMEP vs. intake temperature.

relationship in $V$, $p$ and $T$, and the REFPROP 7.0 is used to calculate the thermodynamic parameters of the Rankine cycle system [16].

Heat transfer equation:

$$\frac{dQ_j}{dt} = \sum_{i}^{3} h_{\text{con}} A_i (T_i - T) \tag{5}$$

where $h_{\text{con}}$ is the heat transfer coefficient, $i = 1, 2, 3$ represent the closed bottom surface of cylinder head, piston top surface and the cylinder wall, respectively. $A_i$ is the heat transfer area of each part and $T_i$ is the wall temperature of each part.

The volume variation of the cylinder can be stated as:

$$V = \frac{\pi D^2}{4}\left(\frac{S}{\varepsilon - 1} + \frac{S}{2}\left(\left(1 + \frac{1}{\lambda}\right) - \cos\left(\frac{\pi}{180}\cdot\varphi\right) - \frac{1}{\lambda}\sqrt{1 - \lambda^2\cdot\sin^2\left(\frac{\pi}{180}\cdot\varphi\right)}\right)\right) \tag{6}$$

$$\frac{dV}{d\varphi} = \frac{\pi^2\cdot D^2\cdot S}{180}\left(\sin\left(\frac{\pi}{180}\cdot\varphi\right) + \frac{\lambda}{2}\frac{\sin\left(\frac{\pi}{180}\cdot 2\varphi\right)}{\sqrt{1 - \lambda^2\cdot\sin^2\left(\frac{\pi}{180}\cdot\varphi\right)}}\right) \tag{7}$$

where $\varepsilon$ is the compression ratio, $D$ the cylinder diameter, $S$ the stroke of piston, $\lambda$ the ratio of connecting rod length with the crank-arm radius, and $\varphi$ the crankshaft angle relative to TDC.

The mass flow rate may be calculated using Eq. (8). In this equation, the working fluid flowing into or out of cylinder can be considered as quasi-one-dimensional flow. The intake and exhaust valve throats can be regarded as orifices whose areas vary with time changing, and we assume that the process is one-dimensional, isentropic and adiabatic flow. The actual mass flow rate equals to the theoretical flow rate multiplied by the flow coefficient $\alpha$.

$$\frac{dm}{dt} = \alpha A\sqrt{2p_1\rho_1}\cdot\psi \tag{8}$$

where $\alpha$ is different in various effective valve flowing areas and varies with crankshaft rotation angle; $A$ the flow area, $\rho_1$, the steam density; and $\psi$, the flow function.

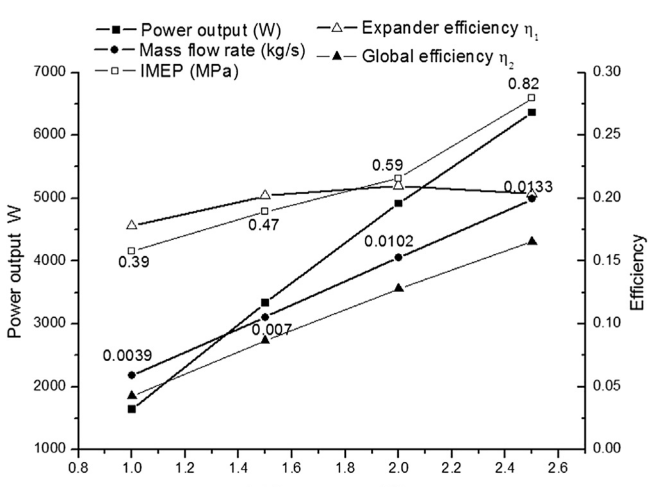


**Fig. 4.** Power output, expander efficiency, global efficiency and mass flow rate, IMEP vs. intake pressure.

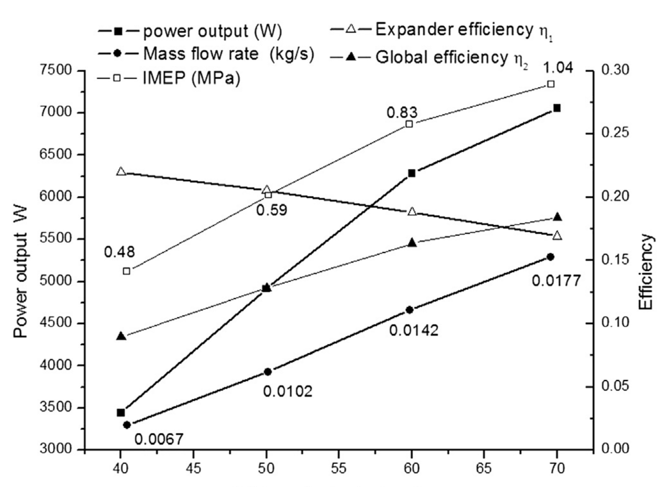


**Fig. 6.** Power output, expander efficiency, global efficiency, mass flow rate and IMEP vs. intake valve closing timing.

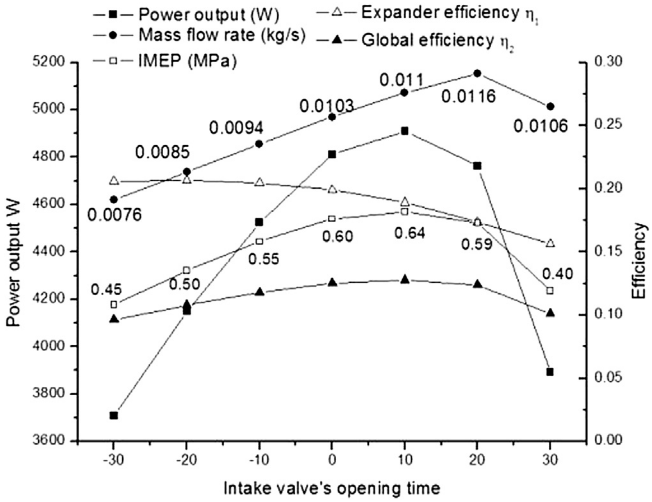


**Fig. 7.** Power output, expander efficiency, global efficiency, mass flow rate and IMEP vs. intake valve's opening time.

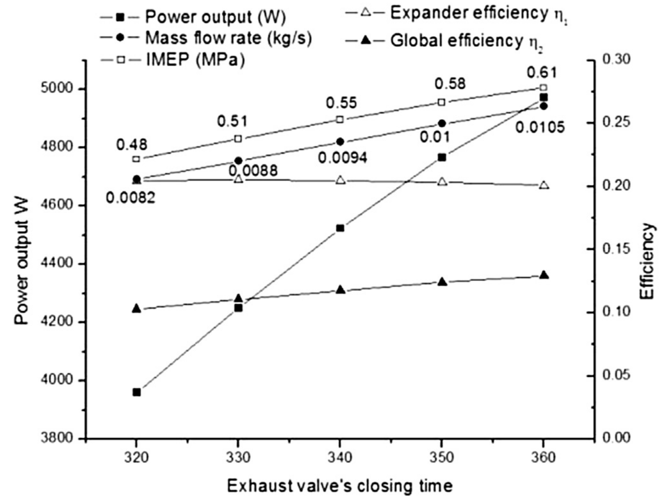


**Fig. 9.** Power output, expander efficiency, global efficiency, mass flow rate and IMEP vs. exhaust valve's closing time.

$$\text{While}\quad \frac{p_2}{p_1} > \left(\frac{2}{k+1}\right)^{\frac{k}{k-1}},\quad \psi = \sqrt{\frac{k}{k-1}\left[\left(\frac{p_2}{p1}\right)^{\frac{2}{k}} - \left(\frac{p_2}{p1}\right)^{\frac{k+1}{k}}\right]} \tag{9}$$

$$\text{While}\quad \frac{p_2}{p_1} < \left(\frac{2}{k+1}\right)^{\frac{k}{k-1}},\quad \psi = \left(\frac{2}{k+1}\right)^{\frac{1}{k-1}}\sqrt{\frac{k}{k+1}} \tag{10}$$

where $k$ is specific heat ratio, $p_1$ and $p_2$ are respectively steam pressure in front of and back of valve.

In order to evaluate the piston expander and global system performance, expander efficiency $\eta_1$ and global system efficiency $\eta_2$ are respectively defined as

$$\eta_1 = \frac{W_{\mathrm{OUT}}}{m_{(\mathrm{ex\_ICE})}(h_{\mathrm{ETS1}} - h_{\mathrm{ETS3}})} \tag{11}$$

$$\eta_2 = \frac{W_{\mathrm{OUT}}}{m_{(\mathrm{ex\_ICE})}(h_{\mathrm{ETS1}} - h_{\mathrm{ambient}})} \tag{12}$$

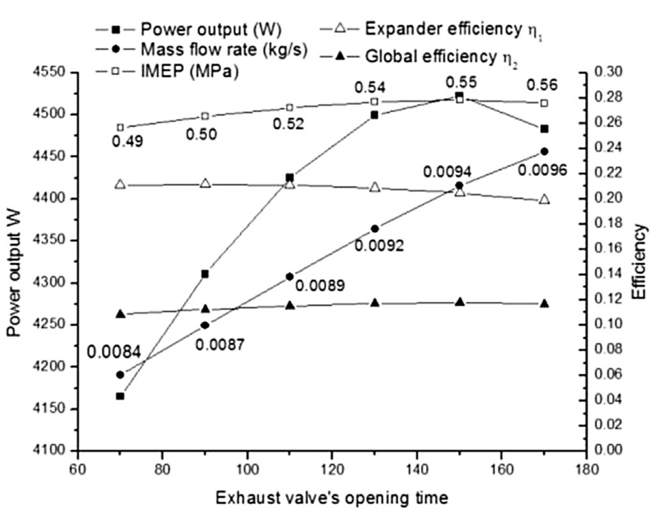


**Fig. 8.** Power output, expander efficiency, global efficiency, mass flow rate and IMEP vs. exhaust valve's opening time.

where $W_{\mathrm{OUT}}$ is the work output of the expander, and $m_{(ex\_ICE)}$ the exhaust mass flow rate of ICE. $h_{\mathrm{ambient}}$, $h_{\mathrm{ETS1}}$and $h_{\mathrm{ETS3}}$ are respectively the specific enthalpies of ICE exhaust at ambient condition, inlet and outlet of heat exchanger (shown in Fig. 14). Therefore, $\eta_1$ gives the information related to the expander efficiency (including steam generation); and $\eta_2$ gives the global efficiency, which is more valuable from the point of view for the whole engine and expander.

### *4.2. Performance simulation of reciprocating piston expander*

The above equations are used to establish the Matlab/Simulink model of the reciprocating piston expander. The model considers the intake and exhaust gas losses, incomplete expansion losses and heat transfer losses except the friction and steam leaks. Then the power output, expander efficiency, global efficiency, the mass flow rate of steam and IMEP (indicated mean effective pressure) can be calculated with this model. The main parameters used in the performance analysis are shown in Table 4.

To enable intelligent comparisons among different operating conditions and design parameters, we shall now analyze the steam engine operating conditions, structure parameters and their relationship in influencing performance capability.

Fig. 3 shows the power output and mass flow rate varying with the expander speed. It can be seen that the power output, mass flow rate and global efficiency increase with the rise of the expander speed, since speed increase causes the steam inlet increasing and leakage losses decreasing in unit time. However, the friction losses increase with expander speed rise, so the expander efficiency decreases with expander speed rise. It is also seen from the figure that IMEP decreases with expander speed rise due to the friction losses increase quickly with the rise of the expander speed. It is seen from Fig. 3 that the global efficiency increases with the expander speed rise, but the expander efficiency and IMEP decrease

**Table 5**
The basic parameters of the designed steam expander.

| | |
|---|---|
| Bore (mm) | 60 |
| Stroke (mm) | 60 |
| The maximum intake valve lift (mm) | 6 |
| The maximum exhaust valve lift (mm) | 6 |
| Intake valve timing | −10 to 40TDC |
| Exhaust valve timing | −30 to 170BDC |

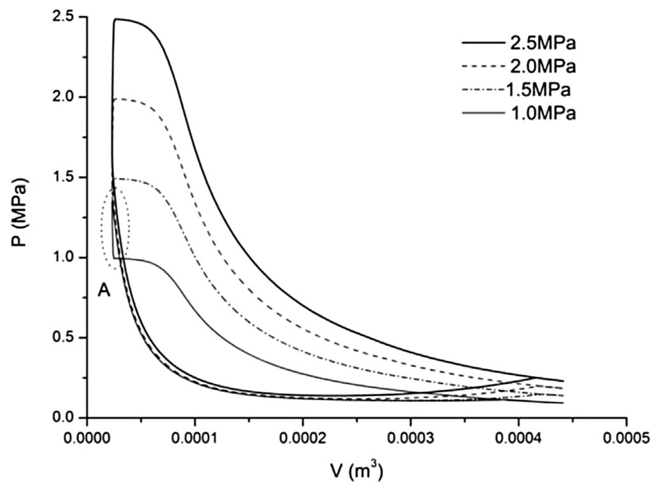


**Fig. 10.** *P*–*V* diagram with different inlet pressure.

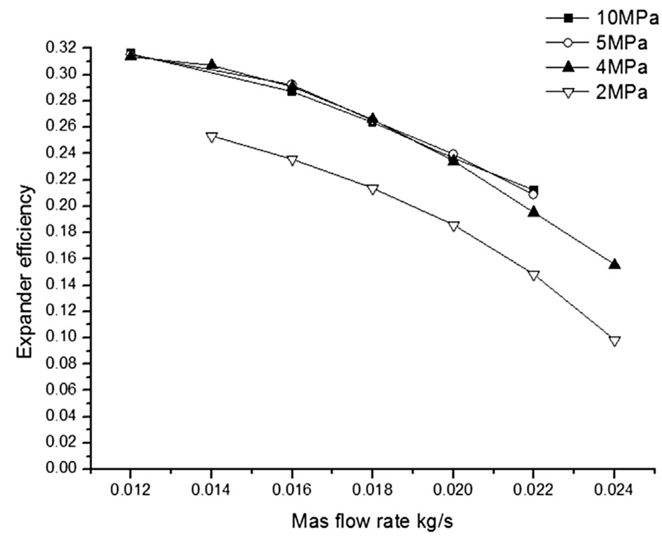


**Fig. 12.** Expander efficiency vs. intake pressure and mass flow rate.

with that. Considering the trade-off between global efficiency and expander efficiency and IMEP, 1400 rpm is chosen as a calculation speed.

*4.2.1. Modification in intake pressure of the steam engine*

The intake pressure rise of the steam engine will lead to a high mass flow rate and thereby a high power output. As indicated in Fig. 4, the power output, mass flow rate and global efficiency increase with the increase of the intake pressure, while the expander efficiency decreases slightly with the increase of the intake pressure when the intake pressure reach 2.0 MPa. Because there is the clearance volume of expander, and at the end of expansion process, the working fluid does not expand fully to the exhaust pressure. As a result, some work will be lost. We called this lost work as incomplete expansion loss. The higher intake pressure results in more incomplete expansion loss. When the intake pressure reach a level, such as 2.0 MPa, the incomplete expansion loss gets high enough, the expander efficiency begins to decrease.

*4.2.2. Modification in intake temperature of the steam engine*

Fig. 5 shows the influence of the intake temperature on the steam engine performance. As indicated in Fig. 5, the power output, global efficiency and expander efficiency increase with the rise of the intake temperature. This can be explained by the enthalpy rise due to the high intake temperature. And the mass flow rate is decreased with the rise of the intake temperature, because the temperature increase will lead to a low steam density and hence to a low mass flow rate and a low IMEP.

*4.2.3. Valve timing influence on the performance of the expander*

Reciprocating steam engine performance is relatively sensitive to the inlet and outlet valve timing. The intake and exhaust valve can be phased in optimum opening and closing timing for large power output and efficiency. Fig. 6 presents the curve of performance vs. intake valve closing timing. It can be seen that the power output, mass flow rate, global efficiency and IMEP increase with the increase of the inlet valve closing timing. The reason for the trends mentioned above is the later intake valve close causing more working fluid flowing into the cylinder during one cycle, so the power output et al. increase, and the expander efficiency decrement is due to the intake losses and incomplete expansion losses when the intake valve closing time delay.

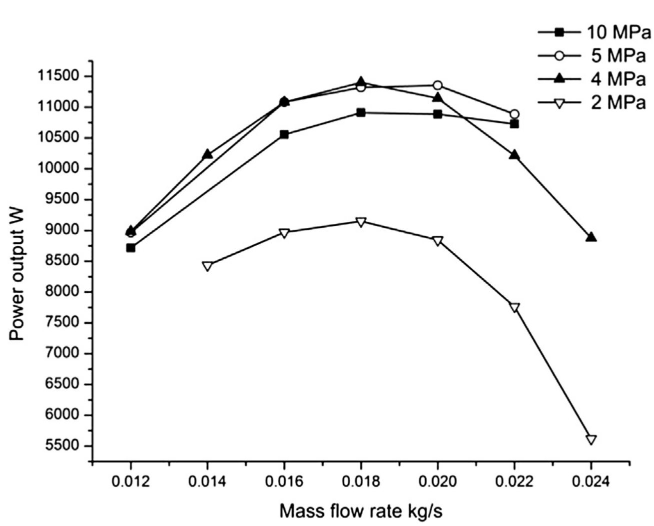


**Fig. 11.** Power output vs. intake pressure and mass flow rate.

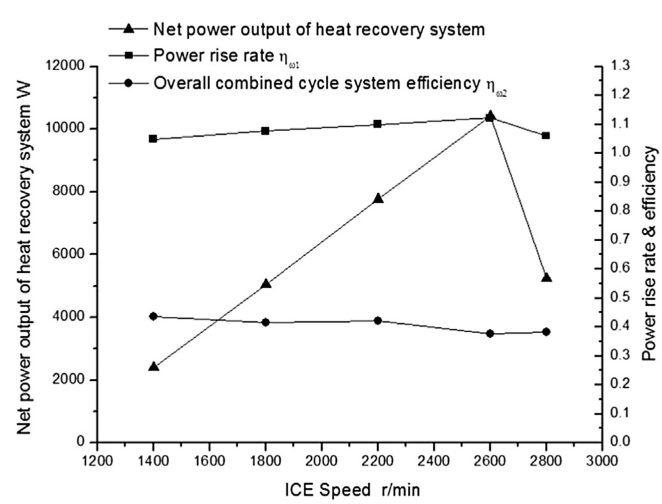


**Fig. 13.** Net power output and power rise rate and combined cycle system efficiency vs. ICE speed.

**Table 6**
Main parameters of ICE.

| | |
|---|---|
| Intake pattern | Turbo charging with inter-cooling |
| Cylinder number | 4 |
| Compression ratio | 17.2 |
| Firing order | 1–3–4–2 |
| Cylinder arrangement | In-line |
| Stroke number | 4 |
| Bore (mm) | 102 |
| Stroke (mm) | 118 |
| Connecting rod length (mm) | 192 |
| Single cylinder displacement (L) | 0.964 |
| Rated speed (r/min) | 2800 |
| Rated power (kW) | 88 |
| Maximum torque (N·m) | 350 |

Fig. 7 shows the relationship of power output, efficiency, mass flow rate and IMEP with the inlet opening timing. It is indicated that there is a suitable inlet opening timing for power output, mass flow rate, global efficiency and IMEP, while the expander efficiency decreases with the rise of inlet opening timing. Therefore, trade-offs between power and efficiency exists with the variation of the inlet opening timing. It needs a balance between output power and expander efficiency in the choice of the inlet valve timing.

The relationship between the exhaust valve timing and the performance are presented in Figs. 8 and 9. A suitable exhaust valve opening timing exists for power output, while with the rise of exhaust valve opening timing, mass flow rate increase, and expander efficiency decrease. As compared to the exhaust opening timing in Fig. 8, the valve closing timing results in less variation of the mass flow rate and expander efficiency (showed in Fig. 9).

### 4.3. *Parameter choice and preliminary design of reciprocating piston expander*

Based on the above analysis, the geometric parameters of the reciprocating piston expander and the operating conditions are determined in this section. For the waste heat recovery of ICE operating in 85 kW/2600 rpm, the basic parameters are chosen and listed in Table 5.

Based on the parameters in Table 5, the indicated diagram (Fig. 10), output power (Fig. 11) and expander efficiency (Fig. 11) are obtained. Fig. 10 shows the *P*–*V* diagram in various intake pressures, it is apparent that the indicated power is proportional to intake pressure. When the inlet pressure decreases to some level (such as 1.0 MPa), a negative work loop is generated on the *P*–*V* diagram as shown in region A. Fig. 10 shows that the inlet pressure must be sufficient for producing the required work.

Figs. 11 and 12 show that an appropriate intake pressure and mass flow rate exist for the expander output and expander efficiency. From the two figures we can see that in order to obtain a high power output, the intake pressure should be 4–5 MPa, and the steam mass flow rate should be 0.015–0.021 kg/s for the reciprocating piston expander.

In order to evaluate the effect of waste heat utilization, it is needed to calculate the net power rise rate and the overall combined cycle system efficiency at various ICE rotation speeds. The net power rise rate $\eta_{w1}$ and the overall combined cycle system efficiency $\eta_{w2}$ are respectively defined in Eqs. (13) and (14).

$$\eta_{w1} = \frac{W_{net} + W_{ICE}}{W_{ICE}} \tag{13}$$

$$\eta_{w2} = \frac{(W_{net} + W_{ICE})}{W_{fuel}} \tag{14}$$

where $W_{ICE}$ is the ICE output power, and $W_{fuel}$ the fuel heat. The net power output $W_{net}$ of recovery system can be expressed as:

$$W_{net} = W - W_{pump} - W_{loss} \tag{15}$$

where $W$ is the power output of expander, $W_{pump}$ the pump power consumption, and $W_{loss}$ the ICE power losses due to exhaust back pressure.

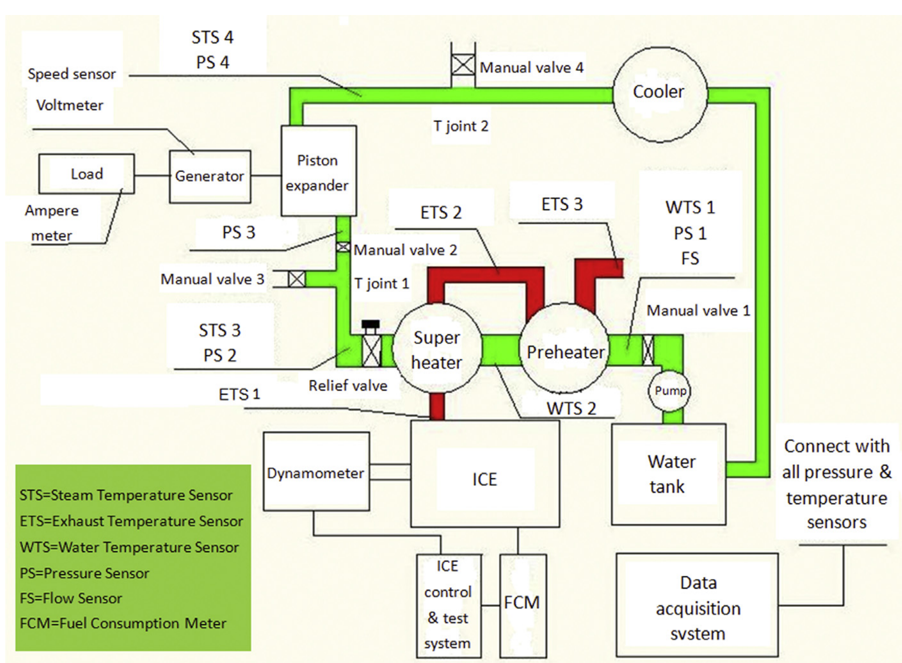


**Fig. 14.** Schematic of the test bench (the red part represents exhaust pipeline of engine, the green part represents steam pipeline), (for interpretation of the references to colour in this figure legend, the reader is referred to the web version of this article).

$$W_{pump} = \frac{W_{pump,ideal}}{\eta_{pump}} \tag{16}$$

where $W_{pump,ideal}$ is pump power when the pump is considered to have isentropic compression process, $\eta_{pump}$ is the pump efficiency. $W_{pump,ideal}$ can be stated as:

$$W_{pump,ideal} = q_w(h_{out} - h_{in}) \tag{17}$$

where $q_w$ is steam mass flow, $h_{in}$ and $h_{out}$ are respectively the specific enthalpy into and out of pump.

We assume that high pressure pump efficiency is 70%, and use the equations above, we can obtain the net power output, power rise rate and efficiency of the overall combined cycle system at various internal combustion engine speeds (such as Fig. 13). After the utilization of waste heat, the power output of overall combined cycle system is increased by 12% at 2600 rpm of ICE.

## 5. Experimental validation

### 5.1. Test bench description

An experimental study was carried out on a reciprocating piston expander in Rankine cycle used to recover waste heat from internal combustion engine. The main parameters of ICE are listed in Table 6. A schematic representation of the test bench is given in Fig.14. The preheater and superheater are heated while ICE exhausts gases flowing through them. The condenser is cooled by water. After passing through the preheater and superheater, the working fluid (overheat steam) enters into the expander which drives an asynchronous electrical machine. Ten bulbs (total 2000 W) are connected in the generator as its load and the generator's load is adjusted by controlling the number of lighted bulbs. Employing the measured voltage and electric current, the whole system's power output can be calculated.

A diaphragm piston-type pump drives the liquid fluid from the condenser to the preheater. The pipes are well insulated thermally from the atmosphere to minimize heat loss to the environment. In order to record the pressure and temperature, as shown in the Fig.14, four pressure sensors and seven temperature sensors were arranged in the whole system. Pressure sensors 1 and 2 are respectively responsible for recording the inlet pressure of the preheater and the outlet pressure of the superheater. Pressure sensors 3 and 4 are arranged in the expander to measure the pressure in inlet and outlet, respectively. The water temperature sensors 1 and 2 are respectively responsible for recording the inlet and outlet temperature of the preheater, and sensors 3 and 4 are respectively responsible for recording the temperatures at superheater and expander outlets.

**Table 7**
Experimental parameters and results.

| | |
|---|---|
| Engine power (kW) | 80 |
| Engine speed (rpm) | 2590 |
| Steam vapor temp (STS) 3(°C) | 157 |
| Intake steam pressure PS. 3(MPa) | 0.35 |
| Expander speed (rpm) | 736 |
| Voltage (V) | 127 |
| Electric current (A) | 2.14 |
| Expander Power (W) | 272 |
| Intake valve timing | −10 to 40 TDC |
| Exhaust valve timing | −30 to 170BDC |
| Heat input of Rankine cycle (kW) | 1.68 |
| Expander efficiency | 16.2% |

### 5.2. Experimental results and analysis

Experiments investigated the characteristics of Rankine cycle system are conducted in the test bench shown in Fig. 15. Tests were performed under 80 kW/2590 rpm of diesel engine. Due to the heat exchanger manufacture deviation from the design parameters, the amount of steam generation is much less than that of prediction, therefore the experimental inlet pressure, mass flow rate and output power of expander are lower than that simulated. The steam preheater inlet pressure (PS1) is 0.382 MPa, and the superheater outlet pressure (PS2) is 0.38 MPa, which indicate that the steam pressure losses are low both in exchanger and connecting pipes. The main parameters measured in experiment are listed in Table 7. Using the parameters of Table 7 in the expander model to calculate expander output power, a 301 W output power is obtained. The calculated power is 10% higher than that measured, mainly due to the friction loss in expander, leakage loss and loss in generator. A *P*–*V* diagram shown in Fig. 16 is obtained using the measured expander cylinder pressure and the crank angle signal.

From the result (Fig. 16) it can be seen that two negative work loops appear. The left one① is as a result of the steam flow back due to the higher cylinder pressure than the inlet pressure of expander when the expander intake valve starts opening. And the right one② is the reason that intake flow is so low that steam over expands in

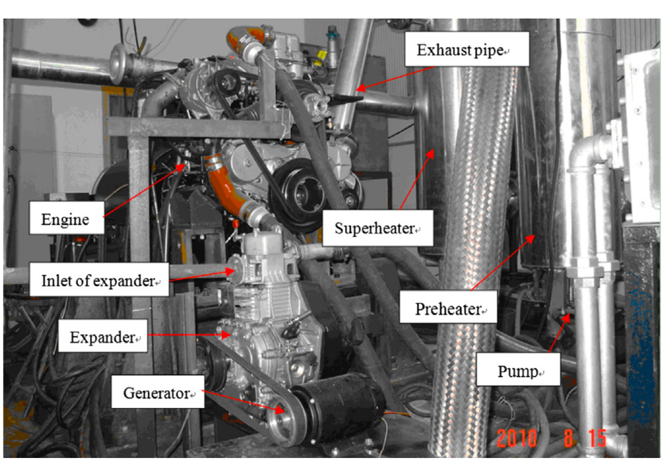


**Fig. 15.** Test bench.

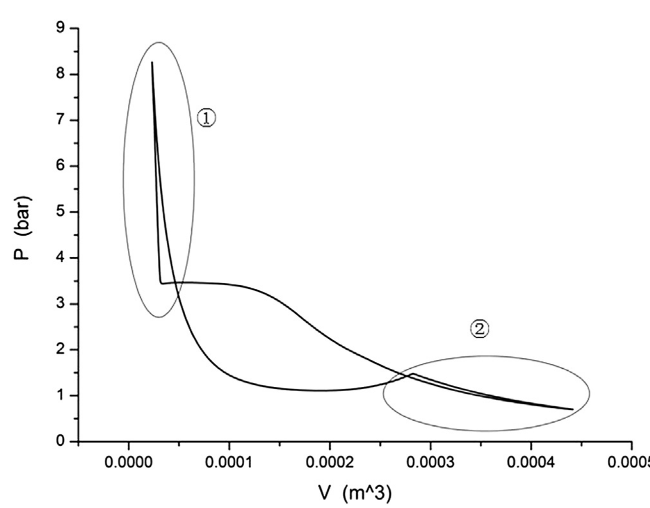


**Fig. 16.** *P*–*V* diagram of expander.

expander, and makes expander do negative work in the end of expansion. Therefore, in order to improve efficiency, the expander inlet pressure should be elevated.

The experimental system should be improved in the following aspects for a high Rankine cycle performance.

1) Design a high pressure and high effective heat exchanger.
2) Increase the pressure ratio of the expander.
3) Use small dynamometer to instead of electric generator to get more accurate measurement for expander power output.
4) Improve air tightness of the experimental system, which will make less losses and efficiencies could reach to high levels.

## 6. Conclusion

The paper highlights the applicability of exhaust heat utilization through secondary fluid power cycles to internal combustion engines and its potential gains. The paper focuses on the performance evaluation and experimental system development of waste heat recovery utilizing reciprocating piston expander. Constructional dimensions and the primary parameters of the heat exchangers are determined by employing a mean temperature difference method. Performances of Rankine cycle operating with reciprocating piston expander were evaluated. Theoretical simulations show that heat recovery and expansion using steam as the working fluid can offer substantial gains in a range of mass flow rate and intake pressure of the expander. A small-scale prototype system based on this concept was developed with guidance from a system model. The proper intake pressure should be 4–5 MPa, and the proper steam mass flow rate should be 0.015–0.021 kg/s for the waste heat recovery of a turbocharged diesel engine (80 kW/2590 rpm). A maximum 12% power output rise is obtained when the diesel engine operates at 80 kW/2590 rpm, expander works at 4 MPa of intake pressure. A test bench is set up with the guidance from the performance simulation results. The test bench performs a given heat duty and respects limitations on shell-side and tube-side pressure drop. However, the expander output power tested is lower than that simulated due to the lower intake steam pressure and lower steam flow rate.

## Acknowledgement

The authors would like to acknowledge the financial support provided by National Basic Research Program of China (973 Program (gs1)) (Grant no. 2011CB707200).

## Nomenclature

| | |
|---|---|
| ICE | Internal combustion engine, / |
| $A_f$ | Flow area, $m^2$ |
| $T$ | Temperature, °C |
| $\rho_1$ | Steam density, $kg/m^3$ |
| $S$ | Entropy, J/kg |
| $\psi$ | Flow function, / |
| $U$ | Internal energy of the steam in the expander, J |
| $k$ | Specific heat ratio, / |
| $Q$ | Heat transferred to the steam in the expander, J |
| $p_1$ | Steam pressure in front of valve, Pa |
| $W$ | Work done by the steam expansion, J |
| $p_2$ | Steam pressure in back of valve, Pa |
| $H$ | Stagnation enthalpy of steam flowing into and out of expander, J/kg |
| $\eta_1$ | Expander efficiency, / |
| $u$ | Specific internal energy of the steam in the expander, J/kg |
| $\eta_2$ | Global system efficiency, / |
| $Q_j$ | Heat losses to the expander walls or to expander head, J |
| $W_{OUT}$ | Work output of the expander, W |
| $p$ | Pressure of the steam in the cylinder, Pa |
| $m_{(ex\text{-}ICE)}$ | Exhaust mass flow rate of ICE, kg/s |
| $V$ | Volume of the steam in the cylinder, $m^3$ |
| $h_{ambient}$ | Specific enthalpy of ICE exhaust at ambient condition, kJ/kg |
| $h_{in}$ | Specific enthalpy entering the cylinder, J/kg |
| $h_{ETS1}$ | Specific enthalpy of ICE exhaust at inlet of heat exchanger, kJ/kg |
| $h_{out}$ | Specific enthalpy discharging the cylinder, J/kg |
| $h_{ETS3}$ | Specific enthalpy of ICE exhaust at outlet of heat exchanger, kJ/kg |
| $m_{in}$ | Mass entering the cylinder, kg |
| $\eta_{w1}$ | Net power rise rate, / |
| $m_{out}$ | Mass discharging the cylinder, kg |
| $\eta_{w2}$ | Overall combined cycle system efficiency, / |
| $m$ | Steam mass in the cylinder, kg |
| $W_{ICE}$ | ICE output power, W |
| $h_{con}$ | Heat transfer coefficient, / |
| $W_{fuel}$ | Fuel heat, W |
| $A_1$ | Heat transfer area of closed bottom surface of cylinder head, $m^2$ |
| $W_{net}$ | Net power output of recovery system, W |
| $A_2$ | Heat transfer area of closed bottom surface of piston top surface, $m^2$ |
| $W$ | Power output of expander, W |
| $A_3$ | Heat transfer area of closed bottom surface of the cylinder wall, $m^2$ |
| $W_{pump}$ | Pump power consumption, W |
| $T_1$ | Wall temperature of closed bottom surface of cylinder head, °C |
| $W_{loss}$ | ICE power losses, W |
| $T_2$ | Wall temperature of closed bottom surface of piston top surface, °C |
| $W_{pump,ideal}$ | Pump power, W |
| $T_3$ | Wall temperature of closed bottom surface of the cylinder wall, °C |
| $\eta_{pump}$ | Pump efficiency, / |
| $\varepsilon$ | Compression ratio, / |
| $q_w$ | Steam mass flow, kg/s |
| $D$ | Cylinder diameter, mm |
| $h_{in}$ | Specific enthalpy into pump, kJ/kg |
| $St$ | Stroke of piston, mm |
| $h_{out}$ | Specific enthalpy out of pump, kJ/kg |
| $\gamma$ | Ratio of connecting rod length with the crank-arm radius, / |
| TDC | Top dead center, / |
| $\varphi$ | Crankshaft angle relative to TDC, / |
| BDC | Bottom dead center, / |
| $\alpha$ | Flow coefficient, / |

## References

[1] Verhelsta Sebastian, Wallnerb Thomas. Hydrogen-fueled internal combustion engines. Progress in Energy and Combustion Science 2006;35:490–527.
[2] Noboru Yamada, Anuar Mohamad Md Nor. Efficiency of hydrogen internal combustion engine combined with open steam Rankine cycle recovering. International Journal of Hydrogen Energy 2010;3:1430–42.
[3] Feng Liming, Gao Wenzhi, Qin Hao, Xie Bixian, Heat recovery from internal combustion engine with Rankine cycle. Power and energy engineering conference (APPEEC); 2010.
[4] Talom Hugues L, Beyene Asfaw. Heat recovery from automotive engine. Applied Thermal Engineering 2009;29(2, 3):439–44.
[5] Patel PS, Doyle EF. Compounding the truck diesel engine with an organic Rankine cycle system. SAE technical paper 1976-760343.
[6] Vaja Lacopo, Gambarotta Agostino. Internal combustion engine (ICE) bottoming with organic Rankine cycles (ORCs). Energy 2010;35:1084–93.

[7] Rody El Chammas. Combined cycle for hybrid vehicles. SAE technical paper 2005-01-1171.
[8] Ho Teng, Gerhard Regner, Chris Cowland. Achieving high engine efficiency for heavy-duty diesel engines by waste heat recovery using supercritical organic-fluid Rankine cycle. SAE technical paper 2006-01-3522.
[9] Arias DA, Shedd TA, Jester RK. Theoretical analysis of waste heat recovery from an internal combustion engine in a hybrid vehicle. SAE technical paper 2006-01-1605.
[10] Srinivasan Kalyan K, Mago Pedro J, Krishnan Sundar R. Analysis of exhaust waste heat recovery from a dual fuel low temperature combustion engine using an organic Rankine cycle. Energy 2010;35:2387–99.
[11] Wang EH, Zhang HG, Fan BY, Ouyang MG, Zhao Y. Study of working fluid selection of organic Rankine cycle (ORC) for engine waste heat recovery. Energy 2011;36:3406–18.
[12] He Maogang, Zhang Xinxin, Zeng Ke, Gao Ke. A combined thermodynamic cycle used for waste heat recovery of internal combustion engine. Energy 2011;36:6821–9.
[13] Badr O, Naik S, O'Callaghan PW, Probert SD. Expansion machine for a low power-output steam Rankine-cycle engine. Applied Energy 1991;39: 93–116.
[14] Badr O, O'Callaghan PW, Hussein M, Probert SD. Rotary Wankel engine as expansion devices in steam Rankine-cycle engines. Applied Energy 1991;39: 59–76.
[15] Badami M, Mura M. Preliminary design and controlling strategies of a small-scale wood waste Rankine cycle (RC) with a reciprocating steam engine (SE). Energy 2009;34:1315–24.
[16] McLinden MO, Klein SA. NIST reference fluid thermodynamic and transport properties – REFPROP version 7.0, NIST standard reference database 23; 2002.